# A Scheme of EDTC Control using an Induction Motor Three-Level Voltage Source Inverter for Electric Vehicles

**R. Zaimeddine†, E.M. Berkouk** and L. Refoufi***

**Abstract** – The object of this paper is to study a new control structure for sensorless induction machines dedicated to electrical drives using a three-level voltage source inverter VSI-NPC. The amplitude and the rotating speed of the flux vector can be controlled freely. The scheme investigated is an Enhanced direct torque control "EDTC" for electric vehicle propulsion. The considered application imposes some constraints which are achieved in EDTC control (fast torque response, optimal switching logic, torque control at zero speed, and large speed control. The results obtained for an induction motor indicate superior performance over the FOC type without need for any mechanical sensor.

**Keywords :** Direct torque control, Electric vehicle, Fast torque response, Field oriented control, Induction motor, Neutral-point clamped, Sensorless vector control, Switching strategy optimisation, Voltage source inverter

## 1. Introduction

There is a growing interest in electric vehicles due to environmental concerns. A suitable closed loop torque controller is required to be used in this type of load, and then a new scheme of direct torque control induction motor for electric vehicles is proposed. Induction motors today are the most widely used ac machines due to the advantageous mix of cost, reliability, and performance.

The rapid development of the capacity and switching frequency of the power semiconductor devices combined with the continuous advancement in power electronics technology have made many changes in static power converter systems and industrial motor drives. The conventional GTO inverters are limited by their dc-link voltage. Hence, the series connections of the existing GTO thyristors have been essential in realizing high voltage and large capacity inverter configurations with the dc-link voltage [1]. The vector control of the induction motor drive has made it possible to be used in applications requiring fast torque control such as traction [2].

In a perfect field oriented control, the decoupling characteristics of the flux and torque are affected highly by the parameter variation in the machine.

This paper describes a control scheme for direct torque and flux control of induction machines fed by a three-level voltage source inverter using a switching table.

In this method, the output voltage is selected and applied sequentially to the machine through a look-up table so that the flux is kept constant and the torque is controlled by the rotating speed of the stator flux. The direct torque control (DTC) is one of the actively researched control schemes that is based on the decoupled control of flux and torque providing a very quick and robust response with a simple control construction in ac drives [3], [4]: The performances of the motor, controller, and drive system developed for this high-performance electric vehicle have been confirmed by simulation.

## 2. Three-Level Inverter Topology

Fig. 1 presents the schematic diagram of a neutral point clamped (NPC) three-level VSI. Each phase of this inverter consists of two clamping diodes, four GTO thyristors, and four freewheeling diodes. Table 1 shows the switching states of this inverter. Since three kinds of switching states exist in each phase, a three level inverter has 27 switching states in total.

A two-level inverter is only able to produce six non-zero voltage vectors and two zero vectors [2]. The representation of the space voltage vectors of a three-level inverter for all switching states forming a two-layer hexagon centred at the origin of the (d, q) plane and a zero voltage vector at the origin of the plane, is depicted in Fig. 2. According to the magnitude of the voltage vectors, we divide them into four groups: the zero voltage vectors ($V_0$),

† Corresponding Author:Dept. of Electrical and Electronic Engineering, "Signals & Systems" Research Laboratory, University of M'hamed Bougara, Boumerdes, Algeria (rabah_zaimeddine@yahoo.fr)
* Dept. of Electrical and Electronic Engineering, "Signals & Systems" Research Laboratory, University of M'hamed Bougara, Boumerdes, Algeria
** Dept. of Electrical Engineering, National Polytechnic School, Algiers, Algeria (em_berkouk@yahoo.fr)
Received 9 July 2007 ; Accepted 13 August 2007

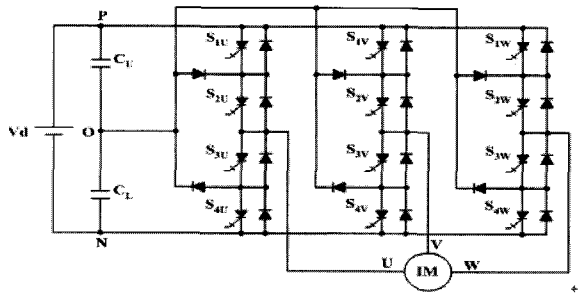


**Fig. 1.** Schematic diagram of a three-level GTO inverter

**Table 1.** Switching states of a three-level inverter

| SWITCHING STATES | $S_1$ | $S_2$ | $S_3$ | $S_4$ | $V_N$ |
|---|---|---|---|---|---|
| P | ON | ON | OFF | OFF | $V_d$ |
| O | OFF | ON | ON | OFF | $V_d/2$ |
| N | OFF | OFF | ON | ON | 0 |

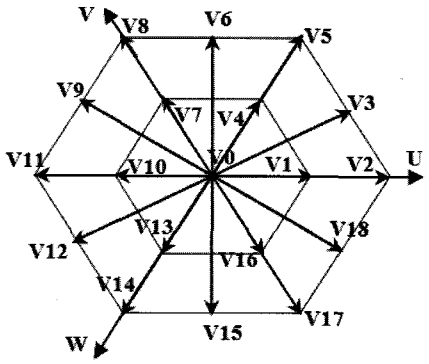


**Fig. 2.** Space voltage vectors of a three-level inverter

the small voltage vectors ($V_1$ , $V_4$ , $V_7$ , $V_{10}$ , $V_{13}$ , $V_{16}$ ), the middle voltage vectors ($V_3$ , $V_6$ , $V_9$ , $V_{12}$ , $V_{15}$ , $V_{18}$ ), and the large voltage vectors ($V_2$ , $V_5$ , $V_8$ , $V_{11}$ , $V_{14}$ , $V_{17}$ ).

The zero voltage vector (ZVV) has three switching states, the small voltage vector (SVV) has two and both the middle voltage vector (MVV) and the large voltage vector (LVV) have only one [1].

## 3. Induction Machine

The torque control of an induction motor can be achieved on the basis of its model developed in a two axis (d, q) reference frame stationary with the stator winding. In this reference frame and with conventional notations, the electrical mode is described by the following equations:

$$\frac{di_{sd}}{dt}=\frac{1}{\sigma T_r L_s}\varphi_{sd}+\frac{p\Omega}{\sigma L_s}\varphi_{sq}-\frac{1}{\sigma}\left(\frac{1}{T_r}+\frac{1}{T_s}\right)i_{sd}-p\Omega i_{sq}+\frac{1}{\sigma L_s}V_{sd} \quad (1)$$

$$\frac{di_{sq}}{dt}=-\frac{p\Omega}{\sigma L_s}\varphi_{sd}+\frac{1}{\sigma T_r L_s}\varphi_{sq}-\frac{1}{\sigma}\left(\frac{1}{T_r}+\frac{1}{T_s}\right)i_{sq}+p\Omega i_{sd}+\frac{1}{\sigma L_s}V_{sq} \quad (2)$$

$$\frac{d\varphi_{sd}}{dt}=V_{sd}-R_s i_{sd} \quad (3)$$

$$\frac{d\varphi_{sq}}{dt}=V_{sq}-R_s i_{sq} \quad (4)$$

The mechanical mode associated to the rotor motion is described by:

$$J\frac{d\Omega}{dt}=\Gamma_{em}-\Gamma_L(\Omega) \quad (5)$$

$\Gamma_L(\Omega)$ and $\Gamma_{em}$ are respectively the load torque and the electromagnetic torque developed by the machine.

## 4. Proposed Direct Torque Control Using a Three-Level Inverter

Basically, DTC schemes require the estimation of the stator flux and torque. The stator flux evaluation can be carried out by different techniques depending on whether the rotor angular speed or (position) is measured or not. For sensorless application, the "voltage model" is usually employed[5]. The stator flux can be evaluated by integration with the stator voltage equation.

$$\varphi_s(t)=\int(Vs-R_s I_s)\,dt \quad (6)$$

This method is very simple, requiring knowledge of the stator resistance only. The effect of an error in Rs is usually neglected at high excitation frequency but becomes more serious as the frequency approaches zero [5].

The deviation obtained at the end of the switching

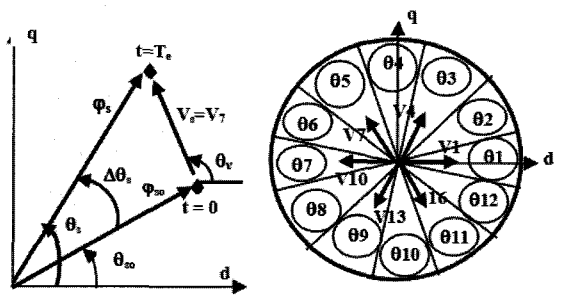


**Fig. 3.** Flux deviation

period Te can be approximated by the first order Taylor Series as below.

$$\Delta\varphi_s \approx V_s.T_e.\cos(\theta_v - \theta_s)$$
$$\Delta\theta_s \approx T_e.\frac{V_s.\sin(\theta_v - \theta_s)}{\varphi_{so}} \quad (7)$$

Consideration is given to the combination of states of switching functions $S_u$, $S_v$, and $S_w$. Fig. 3 shows the adequate voltage vector selection, and we can increase or decrease the stator flux amplitude and phase to obtain the required performance. The electromagnetic torque is estimated from the flux and current information as [2]:

$$\Gamma_{em}=p\,(i_{sq}\varphi_{sd}-i_{sd}\varphi_{sq}) \quad (8)$$

Fig. 4 presents a block diagram of the DTC scheme developed by I. Takahashi [2]. The reference values of flux, $\varphi_s^*$, and torque, $\Gamma_{em}^*$, are compared to their actual values and the resultant errors are fed into a multi-level comparator of flux and torque. The stator flux angle, $\theta_s$ is calculated by:

$$\theta_S=\arctan\frac{\varphi_{sq}}{\varphi_{sd}} \quad (9)$$

and quantified into 12 levels depending on which sector the flux vector falls into. Different switching strategies can be employed to control the torque according to whether the flux has to be reduced or increased.

Each strategy affects the drive behavior in terms of torque and current ripple, switching frequency, and two or four-quadrant operation capability. Assuming the voltage drop ($R_s$ $i_s$) is small, the head of the stator flux $\varphi_S$ moves in

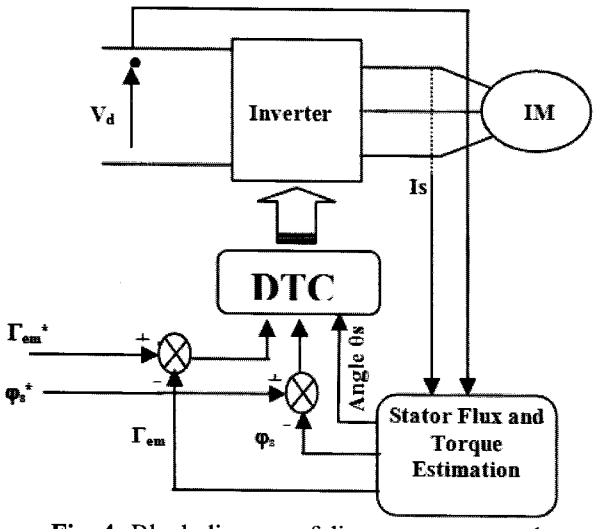


**Fig. 4.** Block diagram of direct torque control

**Table 2.** Selection strategy for four-quadrant operation

| | $\Gamma_{em}$ ↑ | $\Gamma_{em}$ ↓ |
|---|---|---|
| $\varphi_s$ ↑ | $V_{K+1}$ | $V_{K-1}$ |
| $\varphi_s$ ↓ | $V_{K+2}$ | $V_{K-2}$ |

the direction of stator voltage $V_s$ at a speed proportional to the magnitude of $V_s$ according to:

$$\Delta\varphi_S = V_s\,T_e \quad (10)$$

The switching configuration is made step by step, in order to maintain the stator flux and torque within limits of two hysteresis bands, where $T_e$ is the period in which the voltage vector is applied to stator winding. By appropriately selecting the voltage vector step by step, it is then possible to drive $\varphi_s$ along a prefixed track curve [6].

In the case of the three-level inverter, assuming that the stator flux vector is lying in the k-th sector (k=1,2,....12) of the (d, q) plane, and in order to improve the dynamic performance of DTC at low speed and to allow four-quadrant operation, it is necessary to involve the voltage vectors $V_{K-1}$ and $V_{K-2}$ in torque and flux control. In the following, $V_{K-1}$ and $V_{K-2}$ will be denoted "backward" voltage vectors, while "forward" will be used to denote voltage vectors $V_{K+1}$ and $V_{K+2}$. A simple strategy which makes use of these voltage vectors is shown in Table 2.

For steady operating conditions, equations (8) describing the machine torque can be transformed to a sinus function:

$$\Gamma_{elmo} = \Gamma_{max\,o}.\sin 2\gamma_o \quad (11)$$

Where $\Gamma_{maxo}$ *and* $\gamma_o$ are respectively torque and the phase shift angle between the stator and rotor flux vectors.

$$\Gamma_{max\,o} = p.\frac{1-\sigma}{2.\sigma.L_s}.\varphi_{so}^2 \quad ; \quad \gamma_o = \theta_{so} - \theta_{ro} \quad (12)$$

Equations (11) and (12) are established with the assumption that stator flux and rotor are closed values in steady state. For disturbed states, the stator flux angle $\theta_s$ has in practice a fast dynamic mode as compared to the rotor flux angle $\theta_r$. If these two assumptions are valid the effect of stator vector voltage on the electromagnetic torque can be expressed by the first order Taylor expansion as below:

$$\Delta\Gamma_{elm} \approx K_\varphi.\Delta\varphi_s + K_\theta.\Delta\theta_s \quad (13)$$

The sensitivity coefficients Kφ and Kθ are defined by:

$$\begin{cases} K_{\varphi} = \dfrac{d\Gamma_{elm}}{d\varphi_s} = \dfrac{2}{\varphi_{so}}.\Gamma_{elmo} \\ K_{\theta} = \dfrac{d\Gamma_{elm}}{d\theta_s} = 2.\Gamma_{\max o}.\cos 2\gamma_o \end{cases} \quad (14)$$

Using Equations (7), (13) and (14) leads to the following equation:

$$\Delta\Gamma_{elm} = 2.\frac{V_s.T_e}{\varphi_{so}}.\Gamma_{elmo}.\cos(\theta_v - \theta_{so}) + \frac{2.V_s.T_e}{\varphi_{so}}.\sqrt{\Gamma^2_{\max o} - \Gamma^2_{elmo}}.\sin(\theta_v - \theta_{so}) \quad (15)$$

Which shows the feasibility of torque control through a well selected vector voltage $\overline{Vs}$ [7].

## 5. Switching Strategy Proposed For an Enhanced Direct Torque Control

According to this strategy, the stator flux vector is required to rotate in both positive and negative directions. By this, even at very low shaft speed, large negative values of rotor angular frequency can be achieved, which are required when the torque is to be decreased very quickly. Furthermore, the selection strategy represented in Table II allows good flux control to be obtained even in the low speed range. However, the high dynamic performance, which can be obtained using voltage vectors having large components tangential to the stator vector locus, implies very high switching frequency.

For flux control, let the variable $E_{\varphi}$ ($E_{\varphi}=\varphi_s^*- \varphi_s$) be located in one of the three regions fixed by the contraints:

$$E_{\varphi} < E_{\varphi\,min}\ ,\ E_{\varphi\,min} \le E_{\varphi} \le E_{\varphi\,max}\ ,\ E_{\varphi} > E_{\varphi\,max}\ .$$

The suitable flux level is then bounded by $E_{\varphi\,min}$ and $E_{\varphi max}$. Flux control is made by a two-level hysteresis comparator. Three regions for flux location are noted, flux as in fuzzy control schemes, by $E_{\varphi n}$ (negative), $E_{\varphi z}$ (zero), and $E_{\varphi p}$ (positive).

A high level performance torque control is required. To improve the torque control, let the difference ($E_{\Gamma} = \Gamma_{em}^*- \Gamma_e$) belong to one of the five regions defined by the contraints:

$$E_{\Gamma} < E_{\Gamma min2}\ ,\ E_{\Gamma min2} \le E_{\Gamma} \le E_{\Gamma min1}\ ,\ E_{\Gamma min1} \le E_{\Gamma} \le E_{\Gamma max1}\ ,\ E_{\Gamma max1} \le E_{\Gamma} \le E_{\Gamma max2} \text{ and } E_{\Gamma max2} < E_{\Gamma}$$

The five regions defined for torque location are also noted, as in fuzzy control schemes, by $E_{\Gamma nl}$ (negative large), $E_{\Gamma ns}$ (negative small), $E_{\Gamma z}$ (zero), $E_{\Gamma ps}$ (positve small), and $E_{\Gamma pl}$ (positve large). The torque is then controlled by a hysteresis comparator built with two lower bounds and two upper bounds [6].

θ1

| $E_\Gamma$ \ $E_\varphi$ | P | Z | N |
|---|---|---|---|
| PL | 5 | 4 | 8 |
| PS | 3 | 4 | 6 |
| ZE | 0 | 0 | 0 |
| NS | 18 | 0 | 15 |
| NL | 17 | 13 | 14 |

θ2

| $E_\Gamma$ \ $E_\varphi$ | P | Z | N |
|---|---|---|---|
| PL | 5 | 4 | 8 |
| PS | 6 | 7 | 9 |
| ZE | 0 | 0 | 0 |
| NS | 18 | 0 | 15 |
| NL | 2 | 16 | 17 |

θ3

| $E_\Gamma$ \ $E_\varphi$ | P | Z | N |
|---|---|---|---|
| PL | 8 | 7 | 11 |
| PS | 6 | 7 | 9 |
| ZE | 0 | 0 | 0 |
| NS | 3 | 0 | 18 |
| NL | 2 | 16 | 17 |

θ4

| $E_\Gamma$ \ $E_\varphi$ | P | Z | N |
|---|---|---|---|
| PL | 8 | 7 | 11 |
| PS | 9 | 10 | 12 |
| ZE | 0 | 0 | 0 |
| NS | 3 | 0 | 18 |
| NL | 15 | 1 | 2 |

θ5

| $E_\Gamma$ \ $E_\varphi$ | P | Z | N |
|---|---|---|---|
| PL | 11 | 10 | 14 |
| PS | 9 | 10 | 12 |
| ZE | 0 | 0 | 0 |
| NS | 6 | 0 | 3 |
| NL | 5 | 1 | 2 |

θ6

| $E_\Gamma$ \ $E_\varphi$ | P | Z | N |
|---|---|---|---|
| PL | 11 | 10 | 14 |
| PS | 12 | 13 | 15 |
| ZE | 0 | 0 | 0 |
| NS | 6 | 0 | 3 |
| NL | 8 | 4 | 5 |

θ7

| $E_\Gamma$ \ $E_\varphi$ | P | Z | N |
|---|---|---|---|
| PL | 14 | 13 | 17 |
| PS | 12 | 13 | 15 |
| ZE | 0 | 0 | 0 |
| NS | 9 | 0 | 6 |
| NL | 8 | 4 | 5 |

θ8

| $E_\Gamma$ \ $E_\varphi$ | P | Z | N |
|---|---|---|---|
| PL | 14 | 13 | 17 |
| PS | 15 | 16 | 18 |
| ZE | 0 | 0 | 0 |
| NS | 9 | 0 | 6 |
| NL | 11 | 7 | 8 |

θ9

| $E_\Gamma$ \ $E_\varphi$ | P | Z | N |
|---|---|---|---|
| PL | 17 | 16 | 2 |
| PS | 15 | 16 | 18 |
| ZE | 0 | 0 | 0 |
| NS | 12 | 0 | 9 |
| NL | 11 | 7 | 8 |

θ10

| $E_\Gamma$ \ $E_\varphi$ | P | Z | N |
|---|---|---|---|
| PL | 17 | 16 | 2 |
| PS | 18 | 1 | 3 |
| ZE | 0 | 0 | 0 |
| NS | 12 | 0 | 9 |
| NL | 14 | 10 | 11 |

θ11

| $E_\Gamma$ \ $E_\varphi$ | P | Z | N |
|---|---|---|---|
| PL | 2 | 1 | 5 |
| PS | 18 | 1 | 3 |
| ZE | 0 | 0 | 0 |
| NS | 15 | 0 | 12 |
| NL | 14 | 10 | 11 |

θ12

| $E_\Gamma$ \ $E_\varphi$ | P | Z | N |
|---|---|---|---|
| PL | 2 | 1 | 5 |
| PS | 3 | 4 | 6 |
| ZE | 0 | 0 | 0 |
| NS | 15 | 0 | 12 |
| NL | 17 | 13 | 14 |

A switching table is used to select the best output voltage depending on the position of the stator flux and desired action on the torque and stator flux. The flux position in the (d , q) plane is quantified in twelve sectors. Alternative tables exist for specific operation mode. In the switching table for the case of a three-level inverter, it is easily possible to expand the optimal vector selection to include the larger number of voltage vectors produced by the three-level inverter [6]. The appropriate vector voltage

is selected in the order to reduce the number of commutations and the level of steady state ripple.

The switching strategy in the order of the sector θs, is illustrated by each table. The flux and torque control by vector voltage has in nature a desecrate behavior. In fact, we can easily verify that the same vector could be adequate for a set of value of $\theta_s$. The number of sectors should be as large as possible to have an adequate decision.

For this reason, we propose a new approach for direct torque control using a three-level inverter based on twelve regular sectors noted by $\theta_1$ to $\theta_{12}$.

## 6. Modelling the Electric Vehicle System

The motor torque is transmitted to the front wheel via the standard gear box. In braking operation, energy is fed to the battery via the inverter. The high inverter switching frequency (10 KHz) guarantees low noise and good current waveform (small losses due to the current harmonics) [8]. The control strategy is then based on an EDTC induction motor control scheme as indicated in Fig. 5.

The vehicle performance and characteristics are summarized in the Appendix. The considered application imposes two region operations, presented in Fig. 6.

At low speed, from zero to the base speed, a large constant torque is requested. Above the base speed up to the maximum speed a constant power region is requested instead [9].

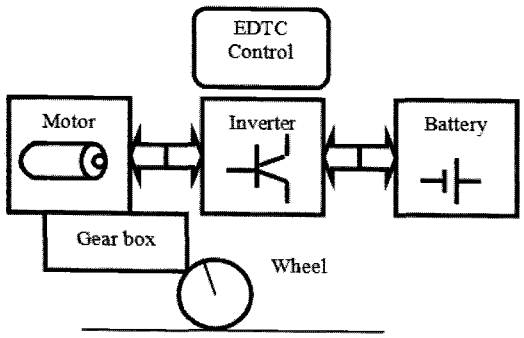


**Fig. 5.** Schematic diagram of propulsion system

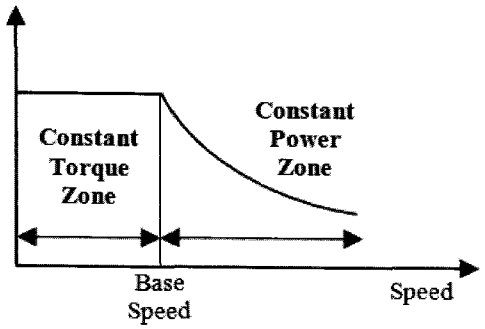


**Fig. 6.** Mechanical characteristics

The functional diagram involves three principal devices consisting of the mechanical part of the vehicle, the power unit, and the electrochemical accumulator. The model used is directly derived from the theories of mechanics and aerodynamics. Fig. 7 illustrates the different forces applied to the vehicle, and can be classified into three types, which are:

Resistance to movement $R_r$. This force is caused by the interaction between the wheel and the road surface, and is given by the relation:

$$R_r = K_r . M . g . \cos\theta \tag{16}$$

$R_r$ : Rolling resistance (N)
$K_r$ : Tabulated value of the rolling resistance coefficient
M : Mass of the vehicle (Kg)
g : Acceleration due to the gravity
θ : Angle between the road surface and the horizontal

The second force is the aerodynamic resistance $R_x$ defined by the Newtonian relation by introducing the aerodynamic coefficient $C_x$ of the vehicle.

$$R_x = \frac{1}{2} . \rho . S . C_x . V^2 \tag{17}$$

$R_x$ : Aerodynamic resistance (N)
ρ : Specific mass of the air
M : Mass of the vehicle (Kg)
V : Speed of the vehicle (m/s)
S : Main frame surface area ($m^2$)
$C_x$ : Aerodynamic coefficient

The resistance to climbing $R_\theta$ is defined by the relation:

$$R_\theta = M . g . \sin\theta \tag{18}$$

The global resistance R is the sum of the resistances acting on the vehicle and the traction force F necessary to move the vehicle forward. It is given by:

$$F = R + (M + m) . \frac{dV}{dt} \tag{19}$$

m: Mass in rotation referred to the wheel (Kg)

The equations linking the wheel and the traction force are:

$$\Omega = \frac{V}{r} \quad and \quad C = r.F \tag{20}$$

r : Radius of the wheel (m)
C : Torque after the gearbox (Nm)
Ω : Speed relation of the transmission shaft (rd/s)

The final equations necessary for determining the speed and the torque of the power unit are those relating to the multiple ration reducer gear:

$$\Omega_m = R_p.\Omega \qquad and \qquad C_m = \frac{C + Cr}{R_p} \tag{21}$$

$R_p$ : Reduction ratio
$C_r$ : Losses torque due to the gear box (function of the temperature of the unit and the rotation speed)

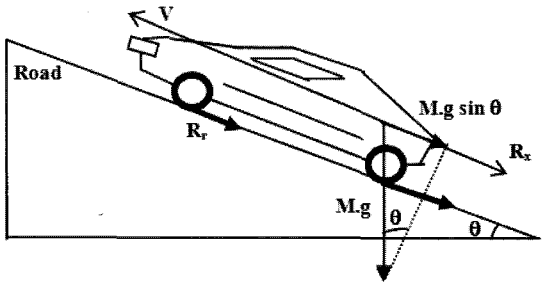


**Fig. 7.** Forces acting on the vehicle

## 7. The Simulation Results

The validity of the proposed DTC algorithm for a three-level voltage source inverter is proved by the simulation results. The parameters of motors are given in the Appendix. The used flux and torque contraints for the EDTC approach are expressed in percent with respect to the flux and torque reference values.

$E_{\varphi max} = 3\%$ , $E_{\varphi min} = -3\%$ , $E_{\Gamma min1} = -0.8\%$ ,
$E_{\Gamma min2} = -3\%$ , $E_{\Gamma max1} = 0.8\%$ , $E_{\Gamma max2} = 3\%$.

The simulation results illustrate both the steady state and the transient performance of the proposed torque control scheme. In the first part, to validate the EDTC system in extended large speed, the machine has been supposed to run at load:

$$\Gamma_L = \left( \frac{\Gamma_{em}}{\Omega_{ref}} - K_f \right).\Omega \tag{22}$$

The FFT of the current waveform of phase (a) is shown in Fig. 8. The phase currents generated by the three-level inverter have low harmonic contents (5.95 % THD).

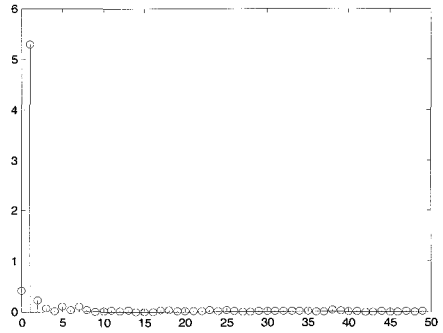

**Fig. 8.** Line current harmonics $I_{sa1}$

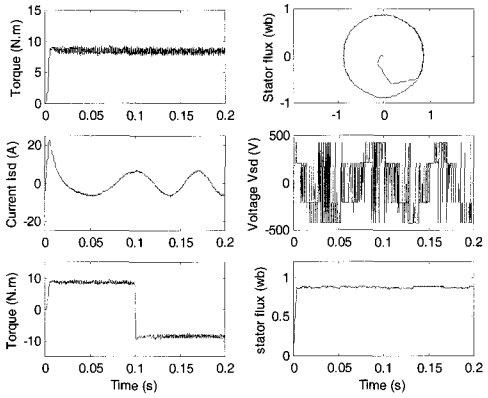


**Fig. 9.** Vector flux locus, torque step response, current $I_{sd}$, voltage $V_{sd}$, torque reverse response, and flux response.

Fig. 9 shows the phase current and flux for steady state and transient operation at 9 N.m with 0.9 Wb. The wave form of the stator current is closed to a sinusoidal signal. The trajectory of the flux is nearly a circle and answers more quickly, (9ms), compared to the flux response in the conventional DTC [6].

The output torque reaches the new reference torque in about 2ms and in this time fast torque response is obtained. A constant flux is maintained during the torque reverse response from + 9 N.m to - 9 N.m and flux command at 0.9 Wb.

Fig. 10 shows the simulation results obtained with EDTC strategy for two modes. In constant torque zone at nominal value of stator flux, reference is from zero to base speed and the constant power zone control with stator flux reference decreases as reverse proportional to the pulsation $\omega_s$ ($\omega_b$=135 rad/s). The simulation results show clearly the operating zones at constant flux and for constant voltage. We note that the stator flux follows the decrease in (1/ $\omega_s$) of the reference $\varphi_{sref}$ at constant voltage. The torque control is optimal and we observe that it is maintained around its reference and follows the law of variation in (1/ $\omega_s^2$) in the constant power zone. During the control process, the maximum torque motor is calculated and plotted.

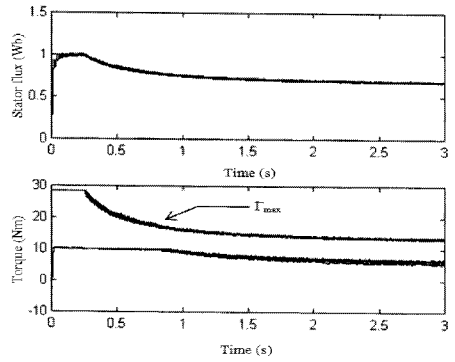


**Fig. 10.** Stator flux response and torque response for optimal control.

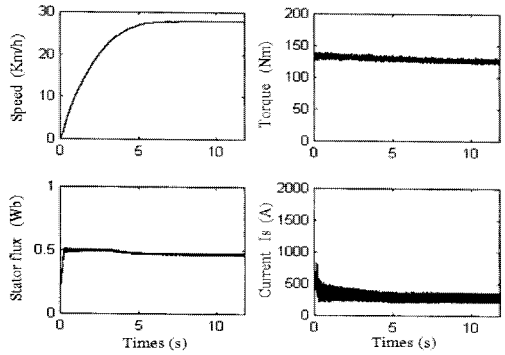


**Fig. 11.** Electric vehicle speed, torque response, stator flux response, and current amplitude Is.

In the second part, we simulate the performances of the EDTC scheme associated to the model of the electric vehicle as load (the simulated system regroups the most important parts: inverter, induction motor, mechanical, aerodynamic, reducing part) for a traction in the case of a flat road in order to observe the evolution of the different sizes as: speed, torque, stator flux, and stator current.

The results given by Fig. 11 indicate that according to this model, for electromagnetic torque reference of 130 Nm and stator flux reference of 0.5 wb, the vehicle reaches the speed of 27km/h in about 7s (note that practically the starting acceleration is in fact limited by the comfort of the travelers). In addition, we note an important peak of the stator current at the starting operation, but it is of short duration. Then its effect is minimized and that oscillates around a middle value of 250 A. It is preferable to make a real optimization of the traction chain with an aspect of minimization of the Joule's losses. In practice, the variation of parameters of the vehicle model imposes a robust control in all conditions.

## 8. Conclusions

The direct torque control DTC was introduced to give a fast and good dynamic torque and can be considered as an alternative to the field oriented control FOC technique, which necessitates generally three feedback loops with PI regulators, a current-regulated PWM converter, and two coordinate transformations. Direct Torque Control (DTC) uses only a couple of hysteresis comparators to perform both torque and flux dynamic control.

The effect of the proposed method has been proved by simulations. It is concluded that the proposed control produces better results for transient and steady state operation.

In this paper, the DTC system using a three-level GTO voltage source inverter is presented, and it is suitable for high-power applications. We enhance the DTC approach by introducing two multi-level hysteresis comparators for flux and torque control. We impose the flux angle detection procedure by defining twelve sectors of space and establish a larger table of knowledge rules with optimal switching strategies.

From this analysis high dynamic performance, good stability and precision are achieved; the results obtained are full of promise to use this system in great power applications as electric vehicle propulsion.

## Appendix

### A. Induction Motor Parameters used in the First Part

Rated power: 1.5 kW
Rated voltage: 220 V
Rated speed: 1420 rpm
Rated frequency: 50 Hz
Rated current: 3.64 A (Y) et 6.31 (Δ)
Stator resistance: 4.85 Ω
Rotor resistance: 3.805 Ω
Stator inductance: 0.274 H
Rotor inductance: 0.274 H
Magnetizing Inductance: 0.258 H
Number of poles: 4
Rotor inertia: 0.031 Kg.m$^2$
Friction Coefficient: 0.008 N.m.s/rd
Vdc = 514 V
Te =100 μs.

### B. Mechanical Characteristics of the Vehicle

Mass of the vehicle: 740 Kg
Density of the air: 1.225 Kg/m$^3$
Drag coefficient: 0.25
Air on good land: 0.015 to 0.03
Frontal projection area: 1.5 m$^2$
Wheel radius: 0.3302m
Inertia of a wheel: 0.5 Kg/ m$^2$
Gearbox: 5 gear-ratio
Battery weight: 28 Kg

Acceleration due to the gravity: $9.81 m/s^2$

### C. Induction Motor Parameters for EV Propulsion

Rated power: 30 kW at 2300 rpm
Maximum torque: 127 Nm
Maximum current: 280 A
Maximum speed: 9000 rpm
Stator resistance: 9 mΩ
Rotor resistance: 7 mΩ
Stator inductance: 1.603 mH
Rotor inductance: 1.5 mH
Magnetizing Inductance: 1.5 mH
Number of poles: 4

## References


[1] Y.H. Lee, B.S. Suh, and D.S. Hyan, "A novel PWM scheme for a three-level voltage source inverter with GTO thyristors". IEEE Trans. on Ind. Appl, vol. 33 2, March\April 1996, pp. 260-268.

[2] I. Takahashi and T. Noguchi, "A new quick-response and high-efficiency control strategy of an induction motor". IEEE Trans. on IA, vol. 22, No. 5, Sept.\Oct. 1986, pp. 820-827.

[3] J.C. Trounce, S.D. Round, and R..M. Duke, "Comparison by simulation of three-level induction motor torque control schemes for electrical vehicle applications". Proc. of international power engineering conference, vol. 1, May 2001, pp. 294-299.

[4] WU. Xuezh and L. Huang, "Direct torque control of three-level inverter using neural networks as switching vector selector". IEEE IAS, annual meeting, 30 September\ 04 October 2001.

[5] D. Casadei, G. Grandi, G. Serra, and A. Tani, "Switching strategies in direct torque control of induction machines". ICEM 94, vol. 2, 1994, pp. 204-209.

[6] R. Zaimeddine and E.M. Berkouk, "A Novel DTC scheme for a three-level voltage source inverter with GTO thyristors". SPEEDAM 2004, Symposium on power electronics, electrical drives, automation & Motion, vol. 2, June, 16th-18th 2004, pp. F1A-9-F1A-12.

[7] F. Bacha, A. Sbai, and R. Dhifaui, "Two Approaches For Direct Torque Control of an Induction Motor". CESA Symposium on control, vol. 1, March 1998, pp. 562-568.

[8] Vasudevan M., and Arumugam, R.; "New direct torque control scheme of induction motor for electric vehicles", Control Conference, 2004. 5th Asian, Vol. 2, 20-23 July 2004, pp. 1377-1383.

[9] S. Manffred and E. Verkehrstechnik, V. Austria, "Electric vehicle with robust sensorless induction motor drive", ICEM 94, Vol. 2, pp. 338-340.


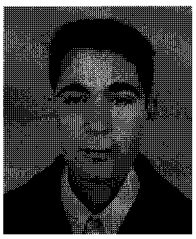


**Rabah Zaimeddine**

He was born in Algiers, Algeria, in 1973. He received his degree in Electrical Engineering from the University of Mouloud Memmeri, Tizi Ouzou, Algeria in 1996. In 1999, he obtained a Magister degree in Electrical Engineering, from the Polytechnic Military School, Algiers, Algeria. In 2007, he obtained his Doctorate of Science from the Polytechnic National School, Algiers, Algeria. Currently, he is a member in the "signal and systems" research laboratory. His current research interests are in the areas of electrical drives, power electronics, electrical machines, and fuzzy logic.



**El Madjid Berkouk**

He was born in Algeria, in 1968. He received the Engineer degree in 1991 in Electrical Engineering from the Polytechnic National School of Algiers, Algeria. In 1993 and 1995, he obtained respectively the Master of Science in ENSEEIHT (Toulouse) and Ph.D in CNAM (Paris). From 1993 to 1996, he was teaching at University of Paris XI. Since 1996, he was with Polytechnic National School, Algiers, Algeria of Algiers as associated Professor and member of process control and renewable energy laboratories. Dr Berkouk is author or co-author of more than hundred of scientific papers. His current research interests are power electronics and electrical drives.


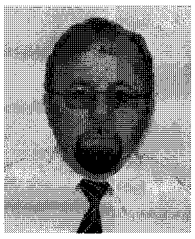


**Prof. L. Refoufi**

He was born in Setif, Algeria in 1953. He obtained the Bachelor's Degree and Master's Degree in 1978 and 1980 respectively from Bradford University, England. In 1991, he obtained the PhD Degree in Electrical Engineering from Newcastle Upon Tyne University, England. He has been a full time teacher at the Institut National d'Electricité et d'Electronique.
since 1981 He is now Professor at the same institution and Director of the ' Signals and Systems' Research laboratory. His current research interests relate to Power Electronics and Electric Drive Systems with particular attention to energy efficiency in general. He is the author of numerous papers in the area of Electric Drives.